Dalton Transactions

Homoleptic complexes of isocyano- and diisocyanobiazulenes with a 12-electron, ligand-based redox capacity

Journal:	*Dalton Transactions*
Manuscript ID	DT-ART-06-2023-001958.R1
Article Type:	Paper
Date Submitted by the Author:	27-Jul-2023
Complete List of Authors:	Connelly, Patrick T; University of Kansas College of Liberal Arts and Sciences, Department of Chemistry Applegate, Jason; University of Kansas College of Liberal Arts and Sciences, Department of Chemistry Maldonado, David A.; University of Kansas College of Liberal Arts and Sciences, Department of Chemistry Okeowo, Monisola K.; University of Kansas College of Liberal Arts and Sciences, Department of Chemistry Henke, Wade C; University of Kansas College of Liberal Arts and Sciences, Department of Chemistry Oliver, Allen; University of Notre Dame Berrie, Cindy; University of Kansas College of Liberal Arts and Sciences, Department of Chemistry Barybin, Mikhail; University of Kansas College of Liberal Arts and Sciences, Department of Chemistry

SCHOLARONE™
Manuscripts

Please do not adjust margins

ARTICLE

Homoleptic complexes of isocyano- and diisocyanobiazulenes with a 12-electron, ligand-based redox capacity

Patrick T. Connelly,[†a] Jason C. Applegate,[†a] David A. Maldonado,[a] Monisola K. Okeowo,[a] Wade C. Henke,[a] Allen G. Oliver,[b] Cindy L. Berrie,*[a] and Mikhail V. Barybin*[a]

Received 00th January 20xx,
Accepted 00th January 20xx

DOI: 10.1039/x0xx00000x

Oligo- and polyazulenes are attractive π-conjugated building blocks in designing advanced functional materials. Herein, we demonstrate that anchoring one or both isocyanide termini of the redox non-innocent 2,2′-diisocyano-6,6′-biazulenic π-linker (**1**) to the redox-active $[Cr(CO)_5]$ moiety provided a convenient intramolecular redox reference for unambiguously establishing that the 6,6′-biazulenic scaffold undergoes a reversible one-step $2e^-$ reduction governed by reduction potential compression/inversion. Treatment of bis(η^6-naphthalene)chromium(0) with six equiv. of 2-isocyano-1,1′,3,3′-tetraethoxycarbonyl-6,6′-biazulene (**6**) or $[(OC)_5Cr(\eta^1$-2,2′-diisocyano-1,1′,3,3′-tetraethoxycarbonyl-6,6′-biazulene)] (**11**) afforded homoleptic Cr(0) complexes **13** and **14** with a $12e^-$ (per molecule) ligand-based reduction capacity at mild $E_{1/2}$ of −1.29 V and −1.15 V vs. $Cp_2Fe^{0/+}$, respectively. The overall reversible redox capacity varies from $15e^-$ for the mononuclear complex **13** to $21e^-$ for the heptanuclear complex **14**. The latter "nanocomplex" has a diameter of *ca.* 5 nm and features seven Cr(0) centers interlinked with six 2,2′-diisocyano-6,6′-biazulenic bridges. The X-ray structure of $[(OC)_5Cr$(2-isocyano-1,1′,3,3′-tetraethoxycarbonyl-6,6′-biazulene)] (**7**) indicated a 43.5° interplanar angle between the two azulenic moieties. Self-assembly of **11** on a Au(111) substrate afforded an organometallic monolayer film of **11** featuring approximately upright orientation of the 2,2′-diisocyano-6,6′-biazulenic linkers, as evidenced by ellipsometric measurements and the RAIR signature of the C_{4v}-symmetric $[(NC)Cr(CO)_5]$ infrared reporter within **11**. Remarkably, comparing the FTIR spectrum of **11** in solution with the RAIR spectrum of **11** adsorbed on Au(111) suggested electronic coupling at a *ca.* 2 nm distance between the Cr(0) and Au atoms linked by the 2,2′-diisocyano-6,6′-biazulene bridge.

Introduction

Isocyanide-terminated arenes and oligoarenes (:C≡N-Ar) have long been a highly sought-after class of π-conducting molecular linkers in the design of advanced organoelectronic materials.[1-10] In an organometallic setting, the isocyanide group constitutes a versatile junction that accommodates metals in a wide range of oxidation states.[1, 11] The σ-donor/π-acceptor characteristics of isocyanide ligands CNR, which are isolobal with carbon monoxide, are tunable through changing the nature of the substituent R. Such tuning can be quantitatively assessed spectroscopically (IR, ^{13}C NMR) via synergistic consideration of the ν_{NC}, $\delta(^{13}CN)$, and $\delta(^{13}CO)$ signatures in $[(OC)_5Cr(CNR)]$ complexes.[12-14]

Until 2006, there were two general routes available for accessing unsymmetrically metalated linear diisocyanoarenes. One approach involves the use of a large (e.g., 10-fold) excess of a diisocyanoarene ligand with respect to a metal reagent to form a coordination adduct featuring one metal-bound and one uncomplexed isocyanide functionalities.[15] This typically gives low yields of the desired mononuclear complexes, results in the formation of unwanted binuclear byproducts, and requires formidable isolation/crystallization protocols.[15] Self-assembly on metallic surfaces, such as Au(111), is the other strategy to induce unsymmetric metalation of linear diisocyanoarenes.[2, 8]

[a] *Department of Chemistry, University of Kansas, Lawrence, KS 66045, USA*
[b] *Department of Chemistry & Biochemistry, University of Notre Dame, Notre Dame, IN 46556, USA*
[†] P.T.C. and J.C.A. contributed equally to this work.
[‡] Electronic Supplementary Information (ESI) available: experimental procedures, spectroscopic and analytical data, details of the electrochemical and crystallographic studies. CCDC 2270007. See DOI: 10.1039/x0xx00000x

Please do not adjust margins

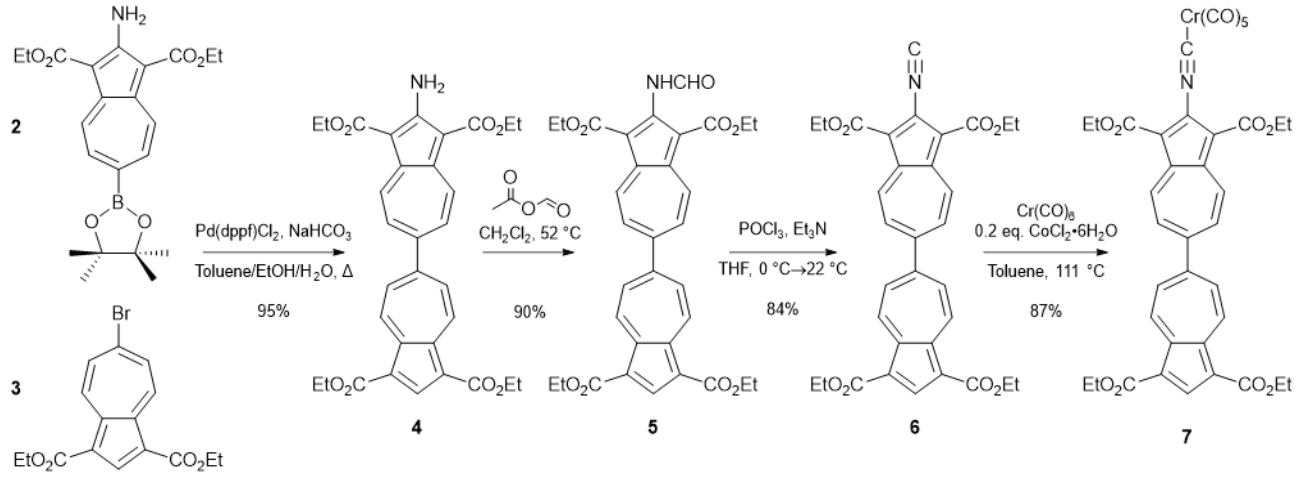

Scheme 2: Synthesis and metalation of the 2-isocyano-6,6′-biazulene ligand **6**.

In 2006, we described an efficient mono- and heterobimetallic complexation of a 2,6-diisocyanoazulenic derivative via controlled stepwise installation and complexation of the isocyanide termini positioned along the molecular axis of the azulenic framework, which is comprised of fused five- and seven-membered sp^2 carbon rings.[16] Later, in 2010, we introduced the first diisocyanobiazulenic π-linker and its self-assembly on metallic gold surfaces.[17] This 2,2′-diisocyano-6,6′-biazulene derivative **1**, shown in Scheme 1, undergoes a reversible one-step 2e^- reduction at a mild potential of −1.02 V vs. $Cp_2Fe^{0/+}$ in $CH_2Cl_2/[^nBu_4N][PF_6]$[17] as a consequence of reduction potential compression/inversion.[18-22] The core of the resulting closed-shell dianion (Scheme 1) may be viewed as a substituted heptafulvalene.[23] Zhuang, Cánovas, Feng *et al.* and Zhuang, Chen *et al.* have recently reported intriguing applications of **1** in designing on-chip microsupercapacitors[24] and quasi-molecular rectifiers.[25] Notably, isocyanide ligands, either free or within a metal complex, that can withstand oxidation or reduction of their substituent without degradation, at least on electrochemical timescales, are extremely scarce (e.g., oxidation of isocyanoferrocene).[26, 27]

Herein, we present a strategy for accessing unsymmetrically anchored linear 2,2′-diisocyano-6,6′-biazulenic π-linkers. We also demonstrate a reversible 12e^- ligand-based reduction

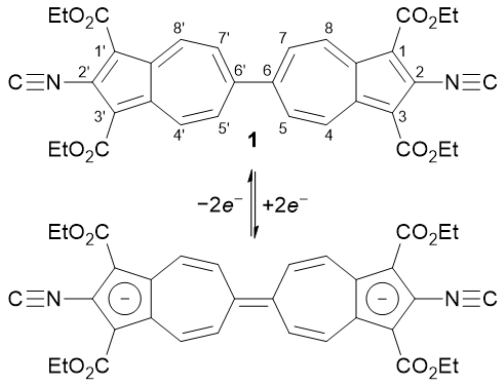

Scheme 1: Atom numbering scheme of the 6,6′-biazulenic scaffold and formation of a heptafulvalene-like motif upon 2e^- reduction of 2,2′-diisocyano-6,6′-biazulene **1**.

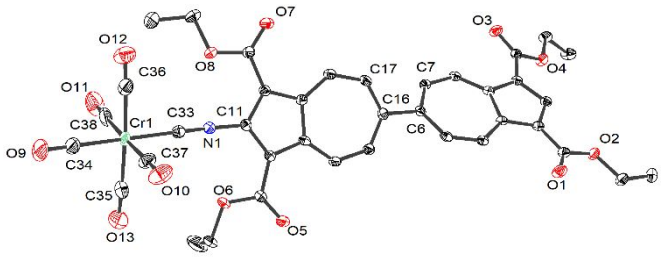

Figure 1: ORTEP diagram (50% thermal ellipsoids) of one of the two crystallographically independent molecules of **7**. Hydrogen atoms and the CH_2Cl_2 solvent of crystallization are omitted for clarity. Selected bond distances (Å) and angles (deg): Cr1-C34 1.887(3), av. Cr1-CO_{cis} 1.905(3), Cr1-C33 1.969(2), C33-N1 1.165(3), N1-C11 1.374(3), C6-C16 1.497(3); Cr1-C33-N1 179.2(2), C11-N1-C33 176.1(2), torsion C7-C6-C16-C17 43.5(3).

capacity[28, 29] of homoleptic octahedral Cr(0) complexes featuring 2-isocyano-1,1′,3,3′-tetraethoxycarbonyl-6,6′-biazulene or [$(OC)_5Cr(\eta^1$-2,2′-diisocyano-1,1′,3,3′-tetraethoxycarbonyl-6,6′-biazulene)] ligands. Given the unusual photophysical properties of azulenic compounds and materials,[30, 31] along with the recently renewed interest in homoleptic low-spin $3d^6$ complexes of isocyanoarenes, particularly in the context of optoelectronic applications,[32, 33] the above species constitute a fundamentally and practically attractive expansion of the $[M(CNAr)_6]$ organometallic platform. Self-assembly of [(-NC)$Cr(CO)_5$]-terminated 6,6′-biazulenic monolayer films anchored on Au(111) surfaces via isocyanide junctions is described as well.

Results and discussion

Assembling the 6,6′-biazulenic core from two differently functionalized (at the 2 position) modules would pave the way to access 6,6′-biazulenes unsymmetrically anchored along their molecular axes.

Our approach to synthesizing a 6,6′-biazulene featuring just one isocyanide terminus is summarized in Scheme 2. Suzuki coupling of the orange-colored 6-pinacolatoborylazulene derivative **2** with the pink 6-bromoazulene derivative **3** afforded orange-red 2-amino-6,6′-biazulene **4** in excellent yield. Subsequent formylation of **4** with acetic-formic anhydride cleanly gave red formamide **5**. $POCl_3$-induced dehydration of **5**

This journal is © The Royal Society of Chemistry 20xx

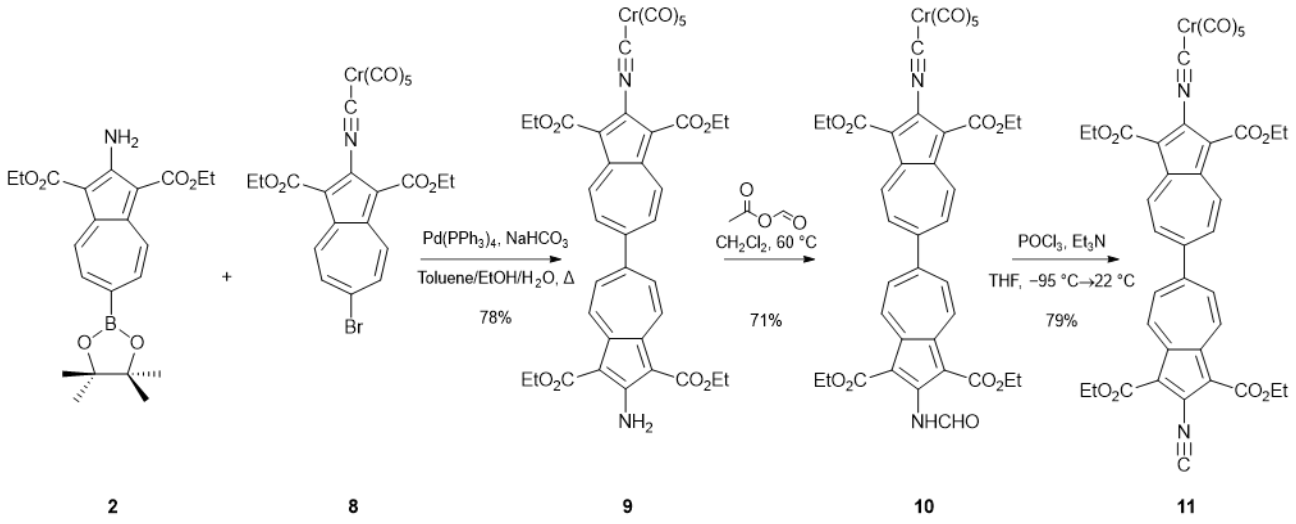

Scheme 3: Synthesis of a mononuclear [$Cr(CO)_5$] complex (**11**) of the 2,2′-diisocyano-6,6′-biazulene ligand **1**.

resulted in the formation of red-purple 2-isocyano-1,1′,3,3′-tetraethoxycarbonyl-6,6′-biazulene **6** in an 84% yield after workup. Treatment of **6** with $Cr(CO)_6$ in refluxing toluene in the presence of $CoCl_2{\cdot}6H_2O$ catalyst provided the maroon-colored organochromium complex **7** in an 87% yield. Notably, we used commercial $CoCl_2{\cdot}6H_2O$ rather than $CoCl_2{\cdot}2H_2O$, which was previously employed by Albers and Coville[34-36] in the catalytic substitution of CO ligands by isocyanides. In principle, complex **7** can also be accessed, albeit in a significantly lower yield of 50%, via photolysis of $Cr(CO)_6$ in THF to form $Cr(CO)_5(THF)$,[13, 16, 17] followed by substitution of the labile THF ligand with isocyanobiazulene **6**.

The solid-state structure of **7**·$(CH_2Cl_2)_{0.375}$ features two crystallographically independent molecules of **7** in the asymmetric unit (Figure S19‡). The interplanar angles between the two azulenic moieties in these two crystallographically unique complexes are 43.5(3)° and 46.2(3)° (Figure Figure 1 and Figure S22‡). The C-C bond length of 1.497(3) Å (C6-C16 in Figure 1) or 1.499(3) Å (C6′-C16′ in Figure S20‡) linking the two seven-membered rings in **7** is indistinguishable from the corresponding C-C bond distance in unfunctionalized 6,6′-biazulene (1.498(2) Å),[37] while being only marginally shorter than the analogous C-C linkage of 1.512(4) Å in **1**.[17] Overall, the metric parameters of the [$(OC)_5Cr(CNC)$] core in **7** are comparable to those in [$(OC)_5Cr(\eta^1$-2,6-diisocyano-1,3-diethoxycarbonylazulene)], in which the diisocyanoazulene ligand is coordinated via the 2-isocyano group,[16] and in [$(OC)_5Cr$(2-isocyano-1,3-diethoxycarbonylazulene)].[14] Of particular note is a pronounced *trans*-effect observed within the octahedral [$(OC)_5Cr(CN)$] core of **7** that makes the Cr-CO_{trans} bond distance 0.014-0.018 Å shorter than the average Cr-CO_{cis} bond length in **7** (Figure Figure 1 and Figure S22‡).

Compound **7** constitutes the first X-ray-structurally characterized 6,6′-biazulene unsymmetrically functionalized with a non-hydrocarbon substituent. The only other unsymmetrically substituted 6,6′-biazulenic motifs that have been crystallographically characterized are within 2,2′:6′,6″-terazulene and 6,2′:6′,6″-terazulene.[38]

Despite unsymmetric functionalization of the 6,6′-

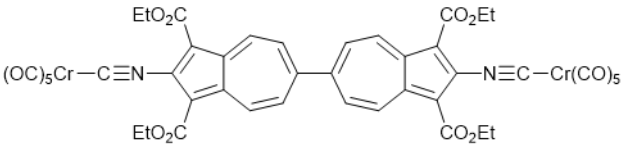

12

Chart 1: Binuclear [$Cr(CO)_5$] complex of the 2,2′-diisocyano-6,6′-biazulene ligand **1**

biazulenyl framework in **6** and **7**, their cyclic voltammograms (CVs) in CH_2Cl_2/[^{n}Bu_4N][PF_6] feature reversible one-step 2e^- reduction of the biazulenic moiety, rather than two separate 1e^- events (Figure S18‡). This is especially evident considering the 1:2 peak current ratio for the reversible $Cr^{0/+}$ wave versus the biazulene$^{0/2-}$ wave in **7** (Figure S18‡). The lack of one of the electron-withdrawing isocyanide termini in **6** compared to diisocyanobiazulene **1** causes a pronounced (140 mV) shift, in the negative potential direction, of the $E_{1/2}$ value associated with reduction of the biazulenic scaffold (Table 1). Upon coordination of **6** to the [$Cr(CO)_5$] moiety to form **7**, the ν_{NC} band undergoes a 9 cm^{-1} hypsochromic shift (Figure S1‡), which is consistent with the σ-donation of the isocyanide's lone pair outweighing the extent of π-back-bonding in **7**. Since the isocyanide C atom's lone pair has a somewhat antibonding character with respect to the C≡N bond,[39] the R-N≡C:→Cr interaction increases the C≡N bond order.[16] In turn, **7** is 20 mV easier to reduce compared to the free isocyanobiazulene **6** (Table 1) because coordination of **6** to the [$Cr(CO)_5$] unit exerts a net electron-withdrawing effect with respect to the isocyanobiazulene ligand.

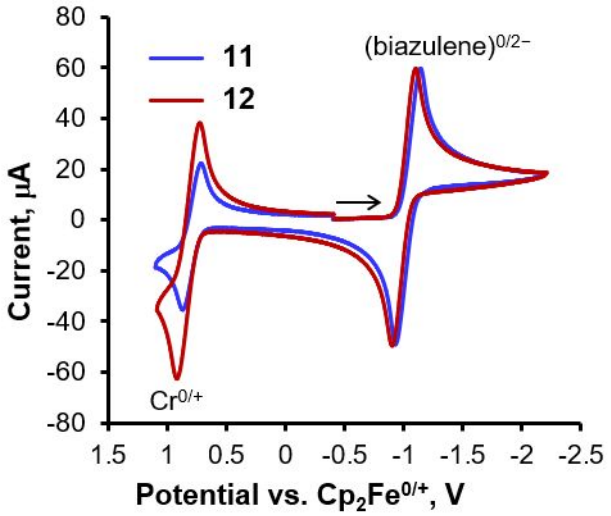

Table 1: Cyclic voltammetry data versus $Cp_2Fe^{0/+}$ for isocyanobiazulene ligands **1** and **6** and their complexes **7**, **11**, and **12** in CH_2Cl_2/[^{n}Bu$_4$N][PF_6].

Compound	Redox couple	$E_{1/2}$ (V)	$\Delta E_{p,c-p,a}$ (mV)	$i_{p,c}/i_{p,a}$
1[17]	Biazulene$^{0/2-}$	−1.02	60	1.0
6	Biazulene$^{0/2-}$	−1.16	170	0.98
7	Biazulene$^{0/2-}$	−1.14	150	1.11
	$Cr^{0/+}$	0.79	120	1.00
11	Biazulene$^{0/2-}$	−1.02	206	0.96
	$Cr^{0/+}$	0.81	156	1.04
12	Biazulene$^{0/2-}$	−1.00	203	0.99
	$Cr^{0/+}$	0.82	180	0.86

Suzuki coupling between 6-pinacolatoborylazulene **2** and the bright orange organochromium derivative of 6-bromoazulene **8** afforded the deep red [$Cr(CO)_5$] complex of 2-isocyano-2'-amino-6,6'-biazulene (**9**, Scheme 3). Formylation of **9** with excess acetic-formic anhydride followed by dehydration of the resulting dark orange formamide **10** gave a 56% combined yield of purple microcrystals of **11**, which is the diisocyanobiazulene **1** (Scheme 1Scheme 1) unsymmetrically metalated at only one of its isocyanide termini (Scheme Scheme 3). The ^{13}C NMR chemical shift for the uncoordinated isocyanide carbon atom in **11** is identical to that previously documented for **1**,[17] whereas the δ(^{13}C) corresponding to the isocyanide C atom coordinated to the Cr(0) center is shifted downfield by *ca.* 6.4 ppm (Figure S8‡). The deep purple complex **12** (Chart 1), which is the binuclear Cr(0) counterpart of the mononuclear complex **11**, was accessed using the procedure previously

Figure 2: Cyclic voltammograms of *ca.* 0.02 M solutions of **11** (blue) and **12** (red) in 0.1 M [^{n}Bu$_4$N][PF_6]/CH_2Cl_2 vs. external $Cp_2Fe^{0/+}$ at 22 °C. Scan rate = 100 mV/s.

reported by us to synthesize [$(OC)_5W]_2$(μ-**1**).[17]

The λ_{max} of the $S_0 \rightarrow S_1$ transition for the free diisocyanobiazulene **1** corresponds to the biazulene-based HOMO→LUMO excitation and occurs at 509 nm (ε = 3.48×10^3 M^{-1} cm^{-1}).[17] Upon complexation of **1** with the [$Cr(CO)_5$] unit to form the mononuclear species **11**, a much more intense band appears at λ_{max} = 485 nm (ε = 29.4×10^3 M^{-1} cm^{-1}), which corresponds to the Cr($d\pi$)→**11**($p\pi$*) metal-to-ligand charge transfer (MLCT) transition. Furthermore, the successive complexation to form the binuclear species **12** is accompanied

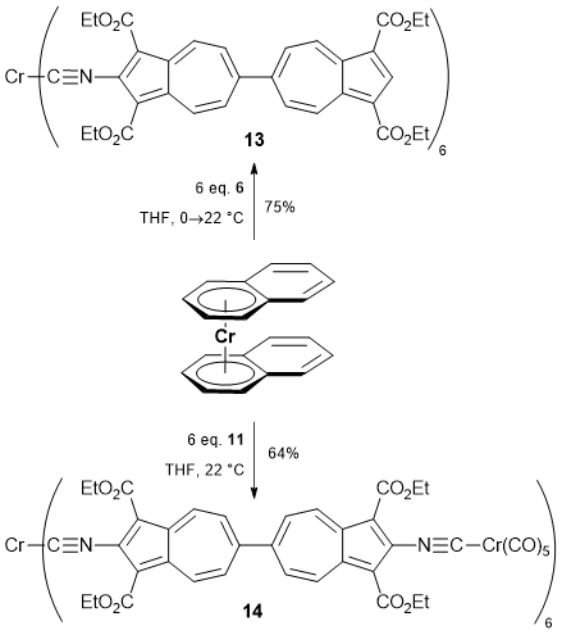

Scheme 4: Syntheses of homoleptic Cr(0) complexes of 2-isocyano-biazulenic ligands **6** and **11**.

by an 895 cm^{-1} redshift of the MLCT band to give λ_{max} = 507 nm (ε = 47.4×10^3 M^{-1} cm^{-1}). The bathochromic shift of the MLCT excitation upon binucleation of **11** to form **12** is consistent with increased conjugation within the π-system that now includes the second [$Cr(CO)_5$] fragment in the binuclear species **12** (Figure S15‡). This bathochromic shift in the MLCT transition for the binucleation process **11**→**12** is approximately half of the 1650 cm^{-1} shift observed for the analogous monoazulenic systems, [$(OC)_5$Cr(η^1-2,6-diisocyano-1,3-diethoxycarbonyl-azulene)]→[$(OC)_5Cr]_2$(μ-η^1:η^1-2,6-diisocyano-1,3-diethoxy-carbonylazulene).[16]

To further appreciate the potential compression/inversion phenomenon associated with the reduction of the 6,6'-biazulenic core of **1**, it is instructive to compare the CV profiles of **11** and **12** (Figure 2, Table 1). The CVs of both **11** and **12** exhibit two distinct redox waves. For **11**, the peak current intensity at *ca.* 0.8 V corresponding to the reversible $Cr^{0/+}$ oxidation of its sole metal center is half of that

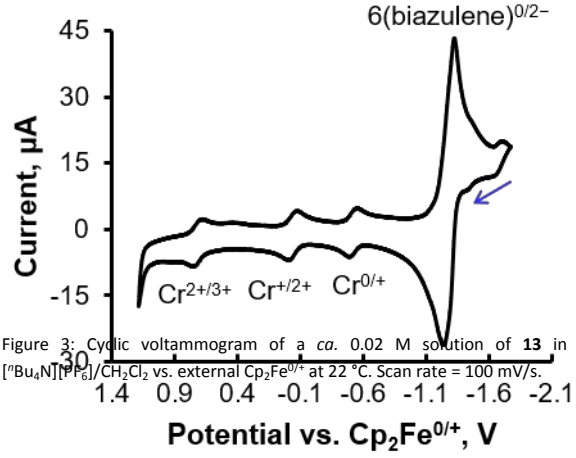

Figure 3: Cyclic voltammogram of a *ca.* 0.02 M solution of **13** in 0.1 M [^{n}Bu$_4$N][PF_6]/CH_2Cl_2 vs. external $Cp_2Fe^{0/+}$ at 22 °C. Scan rate = 100 mV/s.

attributed to the reversible reduction of the biazulenic moiety. On the other hand, the $Cr^{0/+}$ and biazulene$^{0/2-}$ waves have

This journal is © The Royal Society of Chemistry 20xx

essentially identical peak currents for **12**, which features two redox-active chromium termini. Thus, the $[Cr(CO)_5]$ fragments in **11** and **12** effectively serve as reliable intramolecular internal standards for assessing the electrochemical behavior of the diisocyanobiazulene **1**. Notably, the $E_{1/2}$ values of the $Cr^{0/+}$ redox process in **7**, **11**, and **12** (Table 1) are nearly identical to that of 0.78 V observed for $[(OC)_5Cr$(2-isocyano-1,3-diethoxycarbonyl-azulene)].[14]

Treating a THF solution of bis(η^6-naphthalene)chromium(0), a convenient synthon for Cr(0),[40-42] with 6 equiv. of either isocyanobiazulene **6** or $(CO)_5$Cr-capped diisocyanobiazulene **11** under mild conditions afforded the corresponding homoleptic complexes **13** (green) and **14** (black), as illustrated in Scheme 4.

The $\nu_{NC}(T_{1u})$ bands in the FTIR spectra of **13** and **14** in CH_2Cl_2 occur at 1973 cm^{-1} and 1961 cm^{-1}, respectively (Figure S1 and Figure S2‡). This is in accord with the formulation of these coordination compounds as binary Cr(0) complexes of isocyanoarenes exhibiting a substantial extent of Cr(*d*π)→CNR(*p*π*) back-bonding.[42, 43] The 12 cm^{-1} difference between these ν_{NC} values is consistent with the isocyanide ligand **11** being a stronger net π-acceptor compared to **6**. Indeed, incorporation of the $[(NC)Cr(CO)_5]$ substituent at the 2' position of the 2-isocyano-6,6'-biazulenic scaffold extends the conjugation of the ligand's π-system and thereby lowers the energy of **11**'s LUMO compared to that of **6**. Moreover, the electron-withdrawing nature of the $[(NC)Cr(CO)_5]$ moiety contributes to depression of the LUMO energy as well.

We assigned the broad band at λ_{max} = 857 nm (ε = 6.0×10^4 M^{-1} cm^{-1}) in the NIR region of the electronic spectrum of **13** to the Cr(*d*π)→CNR(*p*π*) MLCT transition (Figure S16‡). The Cr(*d*π)→CNR(*p*π*) MLCT[44] involving the central chromium atom in heptanuclear **14** occurs at an even longer wavelength, with λ_{max} ≈ 1000 nm (ε ≈ 10.0×10^4 M^{-1} cm^{-1}, Figure S17‡), which again underscores the lower energy of the LUMO of **11** versus the LUMO of **6**. In addition, in the case of the heptanuclear complex **14**, its electronic spectrum shows an intense band at λ_{max} = 489 nm (ε = 17.8×10^4 M^{-1} cm^{-1}), which corresponds to the Cr(*d*π)→diisocyanobiazulene(*p*π*) MLCT involving six peripheral Cr(0) centers.

The CV profile of **13** features four distinct quasi-reversible redox waves at $E_{1/2}$ = −1.29 V, −0.53 V, −0.04 V, and 0.71 V versus $Cp_2Fe^{0/+}$, with an approximate current intensity ratio of 12:1:1:1, respectively (Figure 3). The lower intensity 1*e*$^-$ waves correspond to the $Cr^{0/+}$, $Cr^{+/2+}$, and $Cr^{2+/3+}$ processes involving the chromium center, akin to those previously documented for other homoleptic $Cr(CNAr)_6$ complexes.[26, 27, 43, 45] The intense 12*e*$^-$ wave reflects 2*e*$^-$ reductions of six biazulenic moieties within **13**. The $E_{1/2}$ value of −1.29 V for this ligand-centered redox couple is 130 mV more negative compared to that observed for the free ligand **6** because of extensive Cr(*d*π)→isocyanobiazulene(*p*π*) back-bonding. Thus, the overall redox capacity of **13** is 15*e*$^-$. The appearance of some structure in the 12*e*$^-$ redox wave at $E_{1/2}$ = −1.29 V is likely caused by minor adsorption of the analyte on the electrode surface.

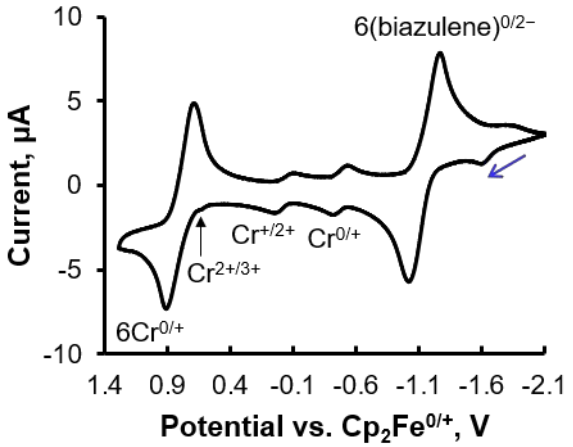

Table 2: Cyclic voltammetry data versus $Cp_2Fe^{0/+}$ for homoleptic complexes **13** and **14** in $CH_2Cl_2/[^nBu_4N][PF_6]$.

Compound	Redox couple	$E_{1/2}$ (V)	$\Delta E_{p,c-p,a}$ (mV)	$i_{p,c}/i_{p,a}$
13	6(Biazulene$^{0/2-}$)	−1.29	85	1.11
	$Cr^{0/+}$	−0.52	65	1.00
	$Cr^{+/2+}$	−0.04	60	0.89
	$Cr^{2+/3+}$	0.71	60	1.00
14	6(Biazulene$^{0/2-}$)	−1.15	250	1.13
	$Cr^{0/+}$	−0.48	110	1.00
	$Cr^{+/2+}$	−0.03	160	1.00
	6($Cr^{0/+}$)	0.80	220	1.07

Compared to that of **13**, the CV of the heptanuclear Cr(0) complex **14** shows an additional quasi-reversible wave at $E_{1/2}$ = 0.80 V ($\Delta E_{p,c-p,a}$ = 220 mV) arising from the $Cr^{0/+}$ redox processes involving the six less electron-rich $[(NC)Cr(CO)_5]$ termini in **14** (Figure 4, Table 2). This intense $Cr^{0/+}$ feature nearly completely obscures the $Cr^{2+/3+}$ redox event at the central chromium atom, for which only the oxidation wave at $E_{p,a}$(ox) = 0.60 V is partially discernable (Figure 4). As expected, the peak currents for the sequential 1*e*$^-$ $Cr^{0/+}$ and $Cr^{+/2+}$ redox events involving the central chromium atom are approximately 1/12 the magnitude of that attributed to the redox activity of the six biazulenic units. Notably, the apparently greater than expected peak current for the peripheral $Cr^{0/+}$ redox process can be attributed to heterogenous *e*$^-$ transfer kinetics in the redox profile of **14**. Indeed, as is evident from Figure 4, the widths of the oxidation

Figure 4: Cyclic voltammogram of a *ca.* 0.02 M solution of **14** in 0.1 M $[^nBu_4N][PF_6]/CH_2Cl_2$ vs. external $Cp_2Fe^{0/+}$ at 22 °C. Scan rate = 100 mV/s.

and reduction waves associated with the peripherally located chromium atoms are smaller than those corresponding to the biazulene$^{0/2-}$ and central chromium atom redox events. Moreover, the $\Delta E_{p,c-p,a}$ peak-to-peak separations for the electrochemical events observed for complex **14** are greater than those documented for complex **13** (Table 2). This is especially pronounced in the two multi-electron waves in Figure 4. This may be attributed to slower electron-transfer kinetics and/or unresolved electronic coupling that results in broadening of the half-waves and increased $\Delta E_{p,c-p,a}$ separation in the case of the *ca.* 5 nm-diameter complex **14**. Altogether, incorporation of the six $[(NC)Cr(CO)_5]$ termini expands the 15*e*$^-$

overall redox capacity of the mononuclear electron reservoir[46-49] **13** to 21e^- in heptanuclear **14**.

Soaking a 1×1 cm^2 gold-coated silicon substrate, featuring preferential Au(111) surface face orientation, for *ca*. 24 hours in a CH_2Cl_2 solution of **11** led to the formation of a self-assembled monolayer (SAM) film of **11** (Figure 5a) with an ellipsometrically determined film thickness of 22±3 Å. This value compares well with the estimated thickness of 24 Å expected for a perfectly upright orientation of the molecules of **11** on the gold surface.[17]

The RAIR absorption profile of **11-Au** is markedly different from that of **11** in solution (Figure 5b,c). The ν_{NC} band attributed to the free isocyanide terminus of **11** in solution phase undergoes a 40 cm^{-1} hypsochromic shift upon chemisorption of **11** on Au(111). This phenomenon arises from the RN≡C:→Au interaction strengthening the N≡C bond and mirrors what has been previously documented for the adsorption of many isocyanoarenes on metallic gold surfaces,[2] including isocyanoazulenes and the diisocyanobiazulene **1**.[17, 50] On the contrary, there is a marginal change in the ν_{NC} value of the band corresponding to the chromium-bound isocyanide group upon

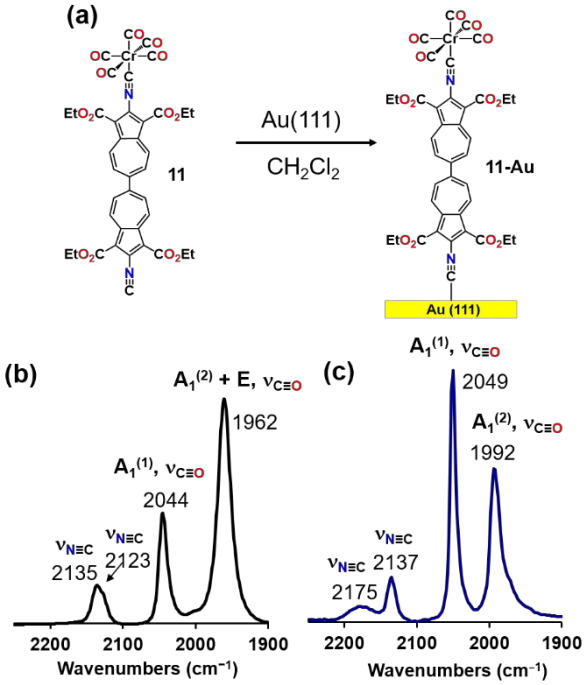

Figure 5: (a) Self-assembly of 2-isocyanobiazulene **11** on Au(111) surface. (b) FTIR spectrum of **11** in CH_2Cl_2. (c) RAIR spectrum of self-assembled monolayer film of **11** on Au(111) (**11-Au**).

SAM formation (2137 vs. 2135 cm^{-1}).

The RAIR spectrum of **11-Au** lacks the intense ν_{CO} band of E symmetry observed in the solution phase because in the upright coordination of **11**, the *cis*-CO oscillators are positioned approximately parallel to the metal surface and, therefore, are forbidden by the surface IR selection rules.[51] The nearly complete vanishing of this ν_{CO}(E) feature uncovers the $\nu_{CO}(A_1^{(2)})$ band which was obscured by the ν_{CO}(E) band in the solution spectrum. Moreover, both ν_{CO} bands of A_1 symmetry, especially $A_1^{(2)}$ ($\Delta\nu_{CO}(A_1^{(2)})$ = 30 cm^{-1}), are shifted to higher energies (Figure 5b,c), signifying a somewhat less pronounced Cr(*d*π)→CO(*p*π*) interaction in the gold surface-bound **11**. Thus, coordination of **11** to the gold surface exerts a measurable reduction in the *net* σ-donor/π-acceptor ratio of the diisocyanobiazulene linker with respect to the $Cr(CO)_5$ moiety at a 2.1 nm distance from the chromium center in this 2,2'-diisocyano-6,6'-biazulene-bridged gold/chromium heterobimetallic system **11-Au**.

Conclusions

In this work, we introduced an efficient synthetic strategy for unsymmetric anchoring of a linear, centrosymmetric diisocyano-6,6'-biazulenic π-linking scaffold. Even when unsymmetrically terminated, the 6,6'-biazulenic moieties still undergo a reversible one-step 2e^- reduction governed by the reduction potential compression/inversion phenomenon. The reduction potential inversion in the electrochemical profile of the 2,2'-diisocyano-6,6'-biazulenic π-linker **1** was unambiguously demonstrated by coordinating it to one or two redox-active $[Cr(CO)_5]$ units, which served as quantitative intramolecular internal references. The bathochromic shift in the Cr(*d*π)→diisocyanobiazulene(*p*π*) MLCT upon binucleation of the mononuclear Cr(0) complex **11** to form the dinuclear Cr(0) complex **12** suggests electronic communication across the *ca*. 2 nm-long 2,2'-diisocyano-6,6'-biazulenic π-bridge. The mononuclear and heptanuclear Cr(0) complexes **13** and **14**, each of which contains six biazulenic moieties, exhibit a reversible 12e^- ligand-based reduction capacity, with their overall molecular redox capacities being 15e^- and 21e^-, respectively.

The C_{4v}-symmetric $[(\text{-NC})Cr(CO)_5]$ moiety served as a powerful remote ν_{CO}/ν_{NC} infrared reporter[12, 13] to demonstrate the terminal-upright coordination mode of the 2-isocyano-6,6'-biazulenic scaffold upon forming its SAM film on metallic gold. Moreover, our RAIR spectroscopic analysis of **11-Au** revealed long-distance (*ca.* 2 nm) electronic interaction between the gold and chromium termini mediated by the 2,2'-diisocyano-6,6'-biazulenic bridge.

Systematic spectroelectrochemical studies pertaining to intermediates generated upon reductive titration of **13** and **14** are currently underway. In addition, the mononuclear and heptanuclear Cr(0) complexes **13** and **14** constitute elementary units in our future construction of 3D metal-organic frameworks involving 6,6'-biazulenic π-linkers.

Data Availability

Crystallographic data for **7** have been deposited as CCDC 2270007. Full experimental details and characterization data are provided in the SI.†

Author Contributions

P.T.C., J.C.A., and D.A.M. carried out the synthetic, characterization, and electrochemical work. A.G.O. and W.C.H. performed the X-ray crystallographic analysis of compound **7**.

This journal is © The Royal Society of Chemistry 20xx

M.K.O. conducted the surface studies. M.V.B. and C.L.B. conceptualized and supervised the work reported herein. M.V.B., P.T.C., and J.C.A. wrote the manuscript. All authors have read, edited, and agreed to the published version of the manuscript.

Conflicts of interest

There are no conflicts to declare.

Acknowledgements

This work was funded by the US National Science Foundation through grant CHE-1808120 to M.V.B. P.T.C. was supported by the Madison and Lila Self Graduate Fellowship at the University of Kansas. D.A.M. is thankful for the support of the Madison and Lila Self Graduate Fellowship and the NSF REU Grant CHE-1560279. J.C.A. was partially supported by the University of Kansas General Research Fund. Support for the NMR instrumentation was provided by NIH Shared Instrumentation Grants (S10OD016360 and S10RR024664), NSF MRI funding (CHE-1625923 and CHE-9977422), and an NIH Center Grant (P20 GM103418). The authors are grateful to Dr. Justin Douglas and Sarah Neuenswander for their assistance with NMR spectroscopic studies. M.V.B. thanks Professor James D. Blakemore of the University of Kansas for many insightful discussions pertaining to the research reported herein.

References

1. M. V. Barybin, J. J. Meyers Jr. and B. M. Neal, in *Isocyanide Chemistry: Applications in Synthesis and Material Science*, ed. V. Nenajdenko, John Wiley & Sons, Weinheim, 2012, ch. 14, pp. 493-529.
2. M. Lazar and R. J. Angelici, in *Modern Surface Organometallic Chemistry*, 2009, DOI: https://doi.org/10.1002/9783527627097.ch13, pp. 513-556.
3. Y. Li, D. Lu, S. A. Swanson, J. C. Scott and G. Galli, *J. Phys. Chem. C*, 2008, **112**, 6413-6421.
4. D. Olson, A. Boscoboinik, S. Manzi and W. T. Tysoe, *J. Phys. Chem. C*, 2019, **123**, 10398-10405.
5. D. Olson, A. Boscoboinik and W. T. Tysoe, *Chem. Commun.*, 2019, **55**, 13872-13875.
6. C. Chu, J. A. Ayres, D. M. Stefanescu, B. R. Walker, C. B. Gorman and G. N. Parsons, *J. Phys. Chem. C*, 2007, **111**, 8080-8085.
7. K. L. Murphy, W. T. Tysoe and D. W. Bennett, *Langmuir*, 2004, **20**, 1732-1738.
8. J. I. Henderson, S. Feng, G. M. Ferrence, T. Bein and C. P. Kubiak, *Inorg. Chim. Acta*, 1996, **242**, 115-124.
9. S. Hong, R. Reifenberger, W. Tian, S. Datta, J. I. Henderson and C. P. Kubiak, *Superlattices Microstruct.*, 2000, **28**, 289-303.
10. M. V. Barybin, *Coord. Chem. Rev.*, 2010, **254**, 1240-1252.
11. L. Malatesta, in *Progress in Inorganic Chemistry*, 1959, DOI: https://doi.org/10.1002/9780470166024.ch5, pp. 283-379.
12. A. E. Carpenter, C. C. Mokhtarzadeh, D. S. Ripatti, I. Havrylyuk, R. Kamezawa, C. E. Moore, A. L. Rheingold and J. S. Figueroa, *Inorg. Chem.*, 2015, **54**, 2936-2944.
13. J. C. Applegate, M. K. Okeowo, N. R. Erickson, B. M. Neal, C. L. Berrie, N. N. Gerasimchuk and M. V. Barybin, *Chem. Sci.*, 2016, **7**, 1422-1429.
14. M. D. Hart, J. J. Meyers, Z. A. Wood, T. Nakakita, J. C. Applegate, N. R. Erickson, N. N. Gerasimchuk and M. V. Barybin, *Molecules*, 2021, **26**, 981.
15. N. L. Wagner, F. E. Laib and D. W. Bennett, *J. Am. Chem. Soc.*, 2000, **122**, 10856-10867.
16. T. C. Holovics, R. E. Robinson, E. C. Weintrob, M. Toriyama, G. H. Lushington and M. V. Barybin, *J. Am. Chem. Soc.*, 2006, **128**, 2300-2309.
17. T. R. Maher, A. D. Spaeth, B. M. Neal, C. L. Berrie, W. H. Thompson, V. W. Day and M. V. Barybin, *J. Am. Chem. Soc.*, 2010, **132**, 15924-15926.
18. D. H. Evans, *Chem. Rev.*, 2008, **108**, 2113-2144.
19. A. J. Fry, *Electroanalysis*, 2006, **18**, 391-398.
20. M. J. Bird, T. Iyoda, N. Bonura, J. Bakalis, A. J. Ledbetter and J. R. Miller, *J. Electroanal. Chem.*, 2017, **804**, 107-115.
21. S. Ito, M. Ando, A. Nomura, N. Morita, C. Kabuto, H. Mukai, K. Ohta, J. Kawakami, A. Yoshizawa and A. Tajiri, *J. Org. Chem.*, 2005, **70**, 3939-3949.
22. S. Ito, T. Okujima and N. Morita, *J. Chem. Soc., Perkin Trans. 1*, 2002, DOI: 10.1039/B203836F, 1896-1905.
23. R. Thomas and P. Coppens, *Acta Crystallogr. Sect. B: Struct. Sci.*, 1972, **28**, 1800-1806.
24. C. Yang, K. S. Schellhammer, F. Ortmann, S. Sun, R. Dong, M. Karakus, Z. Mics, M. Löffler, F. Zhang, X. Zhuang, E. Cánovas, G. Cuniberti, M. Bonn and X. Feng, *Angew. Chem. Int. Ed.*, 2017, **56**, 3920-3924.
25. S. Sun, X. Zhuang, L. Wang, B. Zhang, J. Ding, F. Zhang and Y. Chen, *J. Mater. Chem. C*, 2017, **5**, 2223-2229.
26. T. C. Holovics, S. F. Deplazes, M. Toriyama, D. R. Powell, G. H. Lushington and M. V. Barybin, *Organometallics*, 2004, **23**, 2927-2938.
27. M. V. Barybin, T. C. Holovics, S. F. Deplazes, G. H. Lushington, D. R. Powell and M. Toriyama, *J. Am. Chem. Soc.*, 2002, **124**, 13668-13669.
28. C. Costentin, J.-M. Savéant and C. Tard, *Proceedings of the National Academy of Sciences*, 2018, **115**, 9104-9109.
29. B. de Bruin, P. Gualco and N. D. Paul, in *Ligand Design in Metal Chemistry*, 2016, DOI: https://doi.org/10.1002/9781118839621.ch7, pp. 176-204.
30. S. V. Shevyakov, H. Li, R. Muthyala, A. E. Asato, J. C. Croney, D. M. Jameson and R. S. H. Liu, *The Journal of Physical Chemistry A*, 2003, **107**, 3295-3299.
31. S. Vosskötter, P. Konieczny, C. M. Marian and R. Weinkauf, *Physical Chemistry Chemical Physics*, 2015, **17**, 23573-23581.
32. L. A. Büldt, X. Guo, R. Vogel, A. Prescimone and O. S. Wenger, *J. Am. Chem. Soc.*, 2017, **139**, 985-992.
33. C. Wegeberg, D. Häussinger and O. S. Wenger, *J. Am. Chem. Soc.*, 2021, **143**, 15800-15811.
34. M. O. Albers, N. J. Coville, T. V. Ashworth, E. Singleton and H. E. Swanepoel, *J. Organomet. Chem.*, 1980, **199**, 55-62.
35. M. O. Albers and N. J. Coville, *Coord. Chem. Rev.*, 1984, **53**, 227-259.
36. M. O. Albers, E. Singleton and N. J. Coville, *J. Chem. Educ.*, 1986, **63**, 444-447.

37. Y. Shibuya, K. Aonuma, T. Kimura, T. Kaneko, W. Fujiwara, Y. Yamaguchi, D. Kumaki, S. Tokito and H. Katagiri, *J. Phys. Chem. C*, 2020, **124**, 4738-4746.
38. Y. Yamaguchi, M. Takubo, K. Ogawa, K.-i. Nakayama, T. Koganezawa and H. Katagiri, *J. Am. Chem. Soc.*, 2016, **138**, 11335-11343.
39. R. H. Crabtree, in *The Organometallic Chemistry of the Transition Metals*, John Wiley & Sons, Inc., Sixth edn., 2014, ch. 4, pp. 98-133.
40. M. K. Pomije, C. J. Kurth, J. E. Ellis and M. V. Barybin, *Organometallics*, 1997, **16**, 3582-3587.
41. E. P. Kündig and P. L. Timms, *J. Chem. Soc., Dalton Trans.*, 1980, DOI: 10.1039/DT9800000991, 991-995.
42. M. V. Barybin, V. G. Young and J. E. Ellis, *J. Am. Chem. Soc.*, 2000, **122**, 4678-4691.
43. J. P. Bullock and K. R. Mann, *Inorg. Chem.*, 1989, **28**, 4006-4011.
44. N. Sinha and O. S. Wenger, *J. Am. Chem. Soc.*, 2023, **145**, 4903-4920.
45. R. E. Robinson, T. C. Holovics, S. F. Deplazes, D. R. Powell, G. H. Lushington, W. H. Thompson and M. V. Barybin, *Organometallics*, 2005, **24**, 2386-2397.
46. A. Didier, *Bull. Chem. Soc. Jpn.*, 2007, **80**, 1658-1671.
47. A. Didier, *New J. Chem.*, 2009, **33**, 1191-1206.
48. Y. Morita, S. Nishida, T. Murata, M. Moriguchi, A. Ueda, M. Satoh, K. Arifuku, K. Sato and T. Takui, *Nature Materials*, 2011, **10**, 947-951.
49. S. Muench, A. Wild, C. Friebe, B. Häupler, T. Janoschka and U. S. Schubert, *Chem. Rev.*, 2016, **116**, 9438-9484.
50. D. L. DuBose, R. E. Robinson, T. C. Holovics, D. R. Moody, E. C. Weintrob, C. L. Berrie and M. V. Barybin, *Langmuir*, 2006, **22**, 4599-4606.
51. H. A. Pearce and N. Sheppard, *Surf. Sci.*, 1976, **59**, 205-217.

This journal is © The Royal Society of Chemistry 20xx